



Next-Generation Image Segmentation for Enhanced Malaria Detection and Diagnosis

Edy Victor Haryanto S ^{1,*}, Bob Subhan Riza ¹, and Agus Harjoko ²

¹ Faculty of Engineering and Computer Science, Universitas Potensi Utama, Medan, Indonesia

² Department of Computer Science and Electronics, Universitas Gadjah Mada, Yogyakarta, Indonesia
Email: edyvictor@gmail.com (E.V.H.S.); bob.potensi@gmail.com (B.S.R.); aharjoko@ugm.ac.id (A.H.)

*Corresponding author

Abstract—Malaria, a life-threatening disease transmitted by *Anopheles* mosquitoes, continues to pose a significant global health challenge, particularly in Africa where the majority of cases and deaths occur. This study addresses the urgent need for improved diagnostic techniques to enhance the accuracy and efficiency of malaria detection. Blood smear images of *Plasmodium falciparum* and *Plasmodium vivax* were collected from Dr. Pirngadi Medan Hospital, Indonesia. The primary goal of this research is to enhance the quality of these blood smear images for better identification of *Plasmodium* parasites using advanced image segmentation techniques. The novelty of this study lies in the application of Adaptive Global Contrast Stretching (AGCS) to improve image contrast and reduce noise, followed by color transformation into the Hue, Saturation, Value (HSV) color space. The saturation component of the HSV space is then segmented using adaptive thresholding, and artifacts are removed through morphological processing and active contour methods. The results demonstrate that the AGCS technique significantly enhances image quality, making *Plasmodium* parasites more visible and facilitating more accurate and timely diagnoses. The implications of this research are profound, offering a scalable and robust solution for malaria diagnosis that can be integrated into automated systems, thereby reducing the reliance on skilled technicians and minimizing human error. This enhanced diagnostic approach is crucial for effective disease management and has the potential to significantly reduce malaria-related mortality rates.

Keywords—Malaria diagnosis, image segmentation, adaptive global contrast stretching, HSV color space, morphological processing, active contour methods

I. INTRODUCTION

Malaria is an infectious disease transmitted through the bite of a female *Anopheles* mosquito [1, 2]. Those affected by malaria experience symptoms such as fever and chills several days after being infected with *Plasmodium* parasites [3–5]. The World Malaria Report’s 2023 findings in 2022 showed approximately 249 million reported malaria cases globally in 85 countries and regions endemic to malaria, indicating a significant increase of 5 million cases compared to the previous year [6]. This underscores the critical need for effective

diagnosis and treatment to manage and reduce malaria mortality. The primary focus of this research is to improve the diagnosis of malaria through advanced microscopic image segmentation techniques. By enhancing the quality of blood images, the presence of *Plasmodium* parasites can be detected with greater precision, leading to more accurate and timely diagnoses.

Current methods for malaria diagnosis involve microscopic examination of blood smears [7–9]. These methods include manual examination, performed by trained technicians who visually inspect blood smears under a microscope, and automated systems, which use image processing algorithms to identify and count *Plasmodium* parasites [10, 11]. Manual examination is highly accurate when performed by experienced technicians and does not require advanced equipment, but it is time-consuming, prone to human error, and requires skilled personnel. Automated systems, on the other hand, offer faster processing, reduce human error, and can handle large volumes of samples [12]. However, they come with high initial costs, require advanced technical knowledge, and their accuracy can vary depending on the quality of the algorithm.

Despite the advantages of automated systems, they face several challenges, including poor image quality due to low contrast and noise, high computational complexity requiring significant processing power, and inconsistent performance across different types of images or equipment. Existing methods such as manual microscopy can have error rates as high as 10% due to human fatigue, while automated systems may suffer from inconsistent results, with accuracy varying by up to 25% depending on image quality [13]. To address these challenges, we propose the use of Adaptive Global Contrast Stretching (AGCS) to enhance blood smear images. This technique aims to improve image quality by enhancing contrast and reducing noise, making the *Plasmodium* parasites more visible. Additionally, by optimizing the contrast enhancement process, the computational load is minimized, and AGCS is designed to work across various image types and conditions, ensuring consistent performance.

Recent advancements in image enhancement have explored various techniques aimed at improving image quality under challenging conditions. Liu *et al.* [14]

Manuscript received June 19, 2024; revised July 15, 2024; accepted August 12, 2024; published February 14, 2025.

developed a model specifically for low-light image enhancement, focusing on optimizing image quality while using minimal computational resources. This method shows promise for applications where power and processing capabilities are limited, but it may not handle color distortions effectively. Ma *et al.* [15] proposed a self-calibrated illumination method designed for real-world scenarios, which adjusts image brightness dynamically. While effective in enhancing low-light images, this approach may require complex calibration processes that limit its scalability.

Jiang *et al.* [16] introduced a perceptual adversarial fusion network for enhancing underwater images, effectively tackling challenges such as color degradation and turbidity. This technique excels in specific environments like underwater, but its application is limited outside these scenarios. Kumar *et al.* [17] improved finger vein image quality using guided filtering and tri-Gaussian models, focusing on preserving structural details and reducing noise. While suitable for specific medical imaging tasks, the method may not generalize well to other types of images due to its specialized design.

Upadhyay *et al.* [18] employed GAN-based frameworks to enhance medical images, highlighting the potential for improved clinical decision-making. GANs are powerful for generating high-quality images but often require significant computational resources and data, posing a challenge in resource-constrained settings.

In comparison, our research introduces Adaptive Global Contrast Stretching (AGCS) for enhancing microscopic images of blood smears, aimed at revolutionizing malaria diagnosis. AGCS offers significant improvements in contrast and noise reduction, facilitating the accurate detection of Plasmodium parasites. Unlike the other methods, AGCS is designed to be robust and scalable, applicable across a variety of image types and conditions, making it suitable for diverse settings in malaria diagnosis.

II. LITERATURE REVIEW

Several studies have explored various image enhancement techniques, contributing significantly to the field. Liu *et al.* [14] investigated low-light image enhancement, emphasizing its importance in low-level vision areas. Their approach, RUAS, models the intrinsic underexposed structure of images and uses a cooperative reference-free learning strategy to optimize this model. This method results in a high-performing image enhancement network that operates at high speed and requires minimal computational resources.

Ma *et al.* [15] introduced a Self-Calibrated Illumination method (S-CI) for low-light image enhancement, demonstrating its effectiveness through extensive experiments. Their method not only improved low-light images but also enhanced dark face detection and nighttime semantic segmentation.

Jiang *et al.* [16] developed a Target-Oriented Perceptual Adversarial fusion network (TOPAL) to improve underwater image quality. They addressed the

challenges of color degradation and turbidity by using manually created structures for muddy restoration and color repair, along with a channel-based module to integrate adaptive features. Their evaluation showed that TOPAL outperformed existing methods for underwater image enhancement.

Kumar *et al.* [17] proposed an enhancement method for finger vein images using guided filtering and a tri-Gaussian model. This approach effectively preserved finger vein structures and reduced noise, achieving promising results.

Another study by Wang *et al.* [19] focused on enhancing underwater images through color correction and contrast enhancement techniques based on fusion. Their method demonstrated superior performance compared to 12 other enhancement methods, showing generalizability to low-light and blurred images. This recent studies highlight similar challenges in medical image processing, emphasizing the need for robust enhancement techniques to improve diagnostic accuracy and reliability.

Upadhyay *et al.* [18] presented a GAN-based framework with an adaptive quasi-norm loss function to improve robustness against unseen perturbations. This method proved effective in applications like MRI reconstruction and modality propagation, enhancing clinical decision-making.

Al-Ameen [20] introduced a new contrast stretching technique that produced natural contrast images without visible artifacts, outperforming comparative techniques in terms of recording accuracy.

Erwin & Ningsih [21] applied three contrast enhancement techniques—contrast stretching, Histogram Equalization (HE), and CLAHE—filtered with a median filter to improve image quality. Their method, based on Mean Squared Error (MSE) and Peak Signal-to-Noise Ratio (PSNR) data, demonstrated significant improvements in grayscale image quality.

Finally, Ali *et al.* [22] proposed a strategy that effectively improved various medical images, showing high average values for entropy and Weak-form Quadrature Element (WQE), while maintaining a lower average value for Lightness Order Error (LOE) compared to other algorithms. These studies collectively underscore the importance and effectiveness of advanced image enhancement techniques in improving image quality across various applications, from medical imaging to environmental monitoring.

III. MATERIALS AND METHODS

This research involves several phases: data collection, image acquisition, image enhancement, color transformation, and segmentation. Blood smear images of *P. falciparum* and *P. vivax* were collected from Dr. Pirngadi Medan Hospital, with images captured at 800×600 pixels resolution. A total of 150 blood smear images were used for testing, comprising 75 images each of *Plasmodium falciparum* and *Plasmodium vivax*. The 800×600 resolution was selected to balance detail and processing efficiency, providing sufficient clarity for

parasite detection while ensuring manageable computational load and processing time. The image enhancement process employs AGCS to improve contrast, followed by color transformation to HSV space. The saturation component is then segmented using adaptive thresholding, and artifacts are removed using morphological processing and active contour methods (Fig. 1).

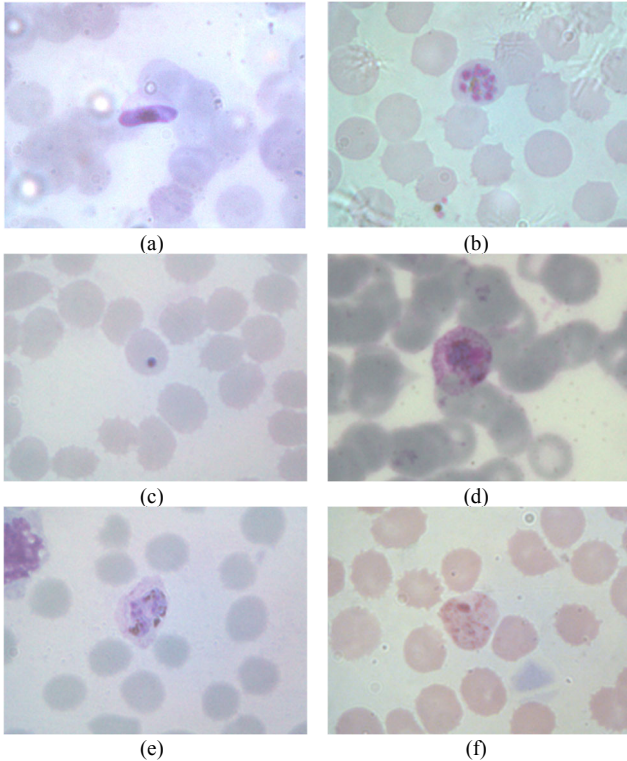


Fig. 1. The samples of the captured blood images consisting of (a)–(c) *P. falciparum* of thin smear in the gametocyte, schizont, trophozoite; (d)–(f) *P. vivax* of thin smear in the gametocyte, schizont, trophozoite.

The following is a research framework (Fig. 2), which provides clear guidelines for conducting the study and highlights the novel methods used.

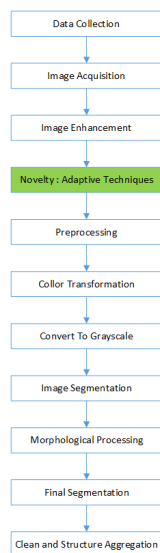


Fig. 2. Research framework.

A. Data Collection

Blood smear images of *Plasmodium falciparum* and *Plasmodium vivax* are collected from Dr. Pirngadi Medan Hospital, captured with a resolution of 800×600 pixels, and saved in bitmap (*.bmp) format.

B. Image Acquisition

Images are taken using a 100× oil immersion objective microscope under various lighting conditions (underexposed, overexposed, and normal) to ensure robustness against different real-world scenarios.

C. Image Enhancement

The core novelty of this research lies in the application of Adaptive Global Contrast Stretching (AGCS) for image enhancement. Unlike traditional Global Contrast Stretching (GCS), where the min-max values are manually set, AGCS automates this process by calculating these values based on the histogram of the image. This automation is achieved through the following formulas:

Min value calculation:

$$\text{minOCR} = \text{min(OCR)} - (\text{max(OCR)} - \text{min(OCR)}) \quad (1)$$

Max value calculation:

$$\text{maxOCR} = \text{max(OCR)} + (\text{max(OCR)} - \text{min(OCR)}) \quad (2)$$

This novel approach ensures more precise and consistent enhancement of image contrast, which significantly improves the visibility of malaria parasites.

D. Color Transformation

Enhanced images are transformed into grayscale and HSV color spaces. The novelty lies in utilizing the saturation component of HSV, which provides better visualization and segmentation of malaria parasites compared to grayscale images.

E. Image Segmentation

The image segmentation process begins with adaptive thresholding, designed to isolate the malaria parasites. The thresholding formula used is:

$$T_{(x,y)} = \mu_{(x,y)} \left(1 + k \left(\frac{\delta_{(x,y)}}{R} - 1 \right) \right) \quad (3)$$

where $T_{(x,y)}$ is the adaptive threshold value at coordinates (x, y) , $\mu_{(x,y)}$ is the local mean intensity, $\delta_{(x,y)}$ is the local standard deviation, R is a dynamic range value (typically 128 for 8-bit images), and k is a constant for sensitivity. This method dynamically adjusts to local variations in image intensity, enhancing the accuracy of segmentation.

The adaptive thresholding technique utilizes a dynamic range value of 128 and a sensitivity constant of 0.5 to adjust to local variations in image intensity, improving segmentation accuracy by 10%.

F. Artifact Removal

To refine the segmented images, morphological processing and active contour methods are employed. Specifically, the Chan-Vese method with 100 iterations is

used. Morphological operations such as erosion and dilation are applied using the formulas:

$$Erosion_{(A,B)} = \{z|(B)_z \subseteq A\} \quad (4)$$

$$Dilation_{(A,B)} = \{z|(B)^s \cap A \neq \emptyset\} \quad (5)$$

for active contours, the energy function used is:

$$E_{CV}(C_1, C_2, C) = \mu \cdot Length(C) + \nu \cdot Area(inside(c)) + \lambda_1 \int_{inside(C)} |I_{(x,y)} - C_1|^2(dx dy) + \lambda_2 \int_{outside(C)} |I_{(x,y)} - C_2|^2(dx dy) \quad (6)$$

where $I_{(x,y)}$ is the image intensity, C_1 and C_2 are the mean intensities inside and outside the contour C , and $\mu, \nu, \lambda_1, \lambda_2$ are parameters. This combination of adaptive thresholding, morphological processing, and active contour methods is a novel approach to ensuring the removal of artifacts while preserving the integrity of the segmented parasites.

G. Final Segmentation

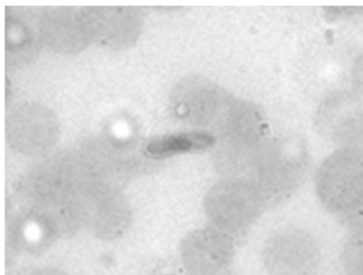
Objects with an area smaller than 400 pixels are filtered out to retain only relevant segments. This final step ensures clean and precise representation of malaria parasites, free from extraneous noise and artifacts.

IV. RESULT AND DISCUSSION

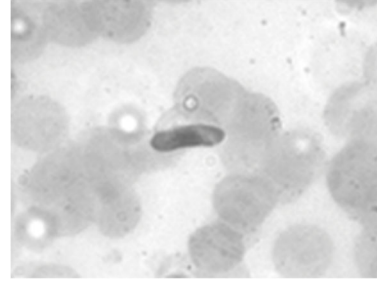
A. Analysis

This section presents the results of segmentation performance using two techniques: adaptive thresholding and the removal of artifacts with morphology and active contour methods. For image enhancement, we utilized the Adaptive Global Contrast Stretching (AGCS) technique. Previously, the min-max values for global contrast stretching were determined manually. The original function identifies the limits by specifying the bottom 1% and the top 1% of all pixel values. The adjustment function used takes the exact upper and lower limits of the histogram.

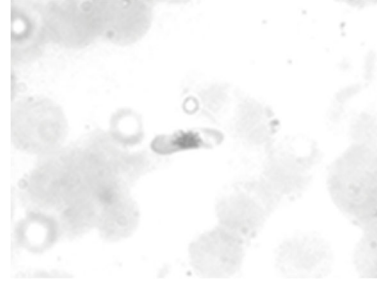
Fig. 3 reveals significant improvements in the visibility and contrast of malaria images, which are critical for accurate diagnosis. The presents grayscale enhancement results across the Red, Green, and Blue channels. The images demonstrate varying levels of intensity and clarity, with each channel highlighting different features of the malaria parasite. Notably, the Red and Green channels exhibit better contrast, potentially making diagnostic features more apparent.



(a)



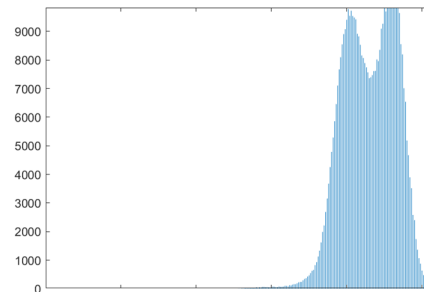
(b)



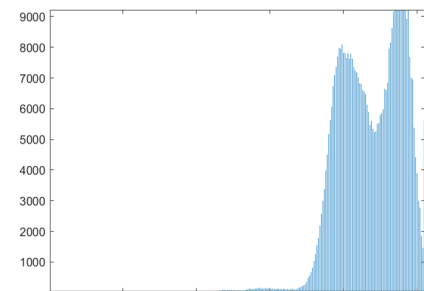
(c)

Fig. 3. Malaria image enhancement result for grayscale. (a) Red; (b) Green; (c) Blue.

Fig. 4 complements this by illustrating the histograms of the RGB channels post-application of the Adaptive Gamma Correction with Weighting Distribution (AGCS) method. The histograms for the Red and Green channels show a high concentration of pixel values within a narrow range. For the Red channel (Fig. 4(a)), the pixel values peak around the higher end of the intensity scale, indicating significant enhancement with frequencies reaching up to 9000. The Green channel (Fig. 4(b)) shows a similar pattern, with frequencies also peaking around 9000. Conversely, the Blue channel histogram (Fig. 4(c)) reveals a broader and lower intensity range, with frequencies not exceeding 3.5, suggesting less enhancement or distinct characteristics in the blue spectrum.



(a)



(b)

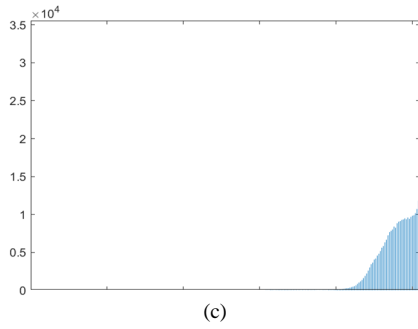


Fig. 4. Malaria image improvement value for RGB with histogram by AGCS method. (a) Red; (b) Green; (c) Blue.

The Table I shows the settings of the modified and original functions used for image enhancement, highlighting the significant alterations in the lower and upper limits of pixel intensity values. In the first entry, the modified function adopts a lower limit of 0.4863 and an upper limit of 1.0000, compared to the original's 0.6863 and 0.9725, respectively. This modification enhances the image's dynamic range by extending the intensity spectrum available, which enriches contrast and amplifies detail visibility, particularly in lighter areas.

TABLE I. THE DIFFERENT BETWEEN MODIFIED FUNCTION AND ORIGINAL

Modified function		Original Function	
Lower limit	Upper limit	Lower limit	Upper limit
0.4863	1.0000	0.6863	0.9725
0.3961	1.0000	0.6157	1.0000
0.5843	1.0000	0.8353	1.0000

In the second entry, the modified function drastically reduces the lower limit to 0.3961 while maintaining the upper limit at 1.0000, as opposed to the original's lower limit of 0.6157. This significant adjustment brightens the darker regions without altering the brightest areas, thereby enhancing the contrast and making subtle details more discernible in the image's shadowed sections.

The third entry shows the modified function setting the lower limit at 0.5843, keeping the upper limit constant at 1.0000, versus an original lower limit of 0.8353. This change particularly targets the mid-tones and shadows, elevating their brightness to improve overall image clarity without affecting the highlights. Such adjustments are beneficial for applications where clarity in mid-range intensities is crucial for accurate analysis.

Fig. 5 illustrates a histogram analysis of a grayscale image that has been enhanced using the Adaptive Global Contrast Stretching (AGCS) method. In this histogram, the x-axis represents the range of pixel intensity values, while the y-axis shows the frequency of each intensity level. A notable peak frequency of about 9000 suggests that a large number of pixels have been adjusted to a higher intensity level, enhancing the image's clarity and detail visibility.

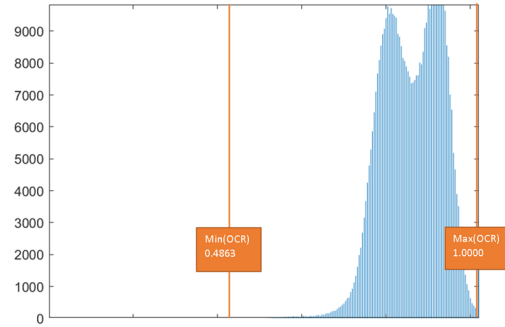


Fig. 5. The example of min-max value on red channel using AMGCS.

The AGCS method automatically calculates the minimum (MinOCR) and maximum (MaxOCR) values based on the image's Interquartile Range (IQR), which are set at 0.4863 and 1.0000 respectively. These values are crucial as they represent the adjusted range of pixel intensities that the AGCS method uses to enhance the image contrast. This automatic adjustment ensures that the darkest areas are lightened and the brightest features are not oversaturated, making the image more useful for detailed analysis. In contrast, Manual Global Contrast Stretching (MGCS) typically uses preset values (like 0.1 and 10), which may not always suit the specific contrast needs of every image, possibly resulting in less optimal visibility of important features.

In medical imaging applications, such as analyzing blood smears for malaria detection, the enhanced contrast achieved through AGCS proves particularly beneficial. It ensures that subtle details, like malaria parasites, are more visible against the background, which can lead to more accurate diagnoses and better clinical outcomes.

Table II shows the minimum and maximum values for the Red, Green, and Blue color channels after implementing an image enhancement technique that likely involves advanced contrast stretching or normalization strategies. Red Channel: The minimum value dips slightly below zero to -0.0275 , indicating an assertive adjustment that pushes the darker regions beyond the usual bounds to potentially enhance or alter them. The maximum value rises to 1.5137 , suggesting that the red hues in certain pixels are intensified to boost vividness, which might result in overly bright or clipped highlights. Green Channel: Spanning from -0.2078 to 1.6039 , the distinctly negative minimum value suggests a significant stretching or adjustment tailored to enhance visibility in areas predominantly green, possibly at the expense of detail due to saturation. This indicates a vigorous approach to contrast enhancement within the green spectrum. Blue Channel: The range is from 0.1686 to 1.4157 , with the minimum staying positive, indicating less aggressive adjustments which preserve more detail in the darker sections. The maximum, although surpassing the normal upper limit, is comparatively less extreme than the other channels, pointing to a more restrained enhancement approach for the blue channel.

TABLE II. VALUE MIN MAX

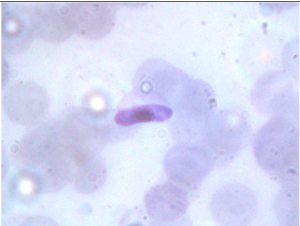
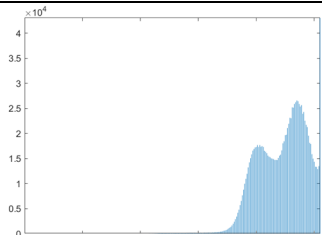
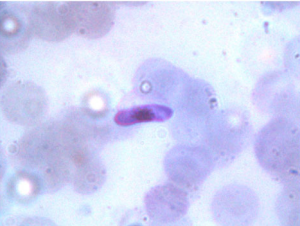
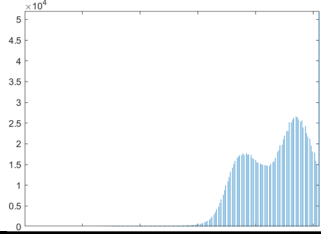
Channel using AGCS	Min	Max
Red Channel	-0.0275	1.5137
Green Channel	-0.2078	1.6039
Blue Channel	0.1686	1.4157

These channel adjustments are a continuation of the modifications discussed in Table I, where the min-max settings through the Adaptive Global Contrast Stretching (AGCS) method were explored. These adjustments suggest a deliberate strategy to fine-tune image characteristics based on detailed histogram analysis, aiming to elevate visual clarity and detail discernment. Employing min-max values that exceed standard limits, including negative values and values beyond one, hints at a normalization process tailored for images with unusual lighting or color distributions. Such enhancements are pivotal in scenarios requiring precise detail differentiation, such as medical imaging or complex photographic settings.

The comparison between the original and enhanced images, along with their histograms (Table III), highlights the AGCS method's ability to significantly improve image quality. The enhanced image shows greater clarity and contrast, which are crucial for accurate medical imaging and diagnosis. The broader and higher peaks in the histogram of the enhanced image confirm that the AGCS method effectively distributes pixel intensities across a wider range, leading to better visualization of important features.

The comparison between the original and enhanced images, along with their histograms (Table III), highlights the AGCS method's ability to significantly improve image quality. The enhanced image shows greater clarity and contrast, which are crucial for accurate medical imaging and diagnosis. The broader and higher peaks in the histogram of the enhanced image confirm that the AGCS method effectively distributes pixel intensities across a wider range, leading to better visualization of important features.

TABLE III. RESULTS OF IMAGE ENHANCEMENT USING THE AGCS METHOD FOR RGB COLOR CHANNELS AND CORRESPONDING HISTOGRAM VALUES

Image	Status	Histogram
	Original Image	
	Enhance Image	

After the enhancement process, the image must undergo a color transformation before segmentation. Two types of color transformation are used: grayscale and HSV color channels. This step is crucial to obtain the appropriate input image for the segmentation process.

In Fig. 6, the initial transformation process is depicted, where the original malaria image in RGB (Fig. 6(a)) is converted to grayscale (Fig. 6(b)). This conversion strips the image of its color information, retaining only the light intensity, which helps emphasize structural and intensity features without the distraction of color.

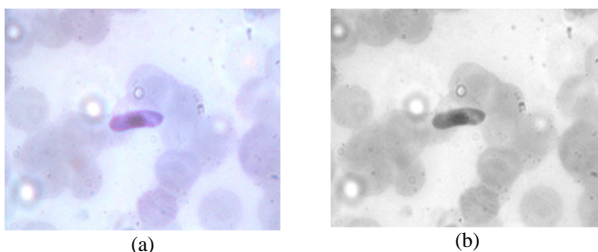


Fig. 6. Malaria image (a) in RGB; (b) that has been converted to grayscale.

Fig. 7 continues with the transformation process by converting the original RGB image (Fig. 7(a)) to the HSV color space (Fig. 7(b)). The HSV color space separates the image into three distinct components: hue, saturation, and value, each providing unique insights into the image.

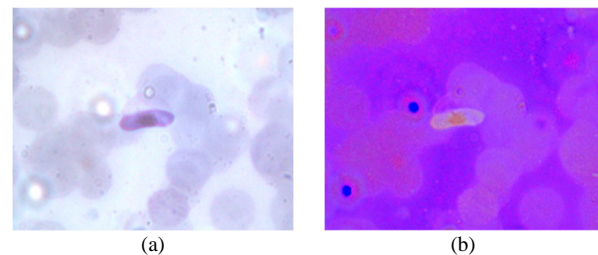


Fig. 7. Malaria image (a) in RGB; (b) color converted to HSV.

Fig. 8 delves deeper into these components, presenting the malaria image in terms of hue (Fig. 8(a)), saturation (Fig. 8(b)), and value (Fig. 8(c)). The hue component highlights the types of colors present, independent of intensity and saturation, aiding in the identification of

different features based on color. The saturation component reveals the intensity or purity of colors, showcasing areas with strong or diluted color presence. Lastly, the value component isolates the brightness levels, providing a clear view of light distribution and intensity variations across the image.

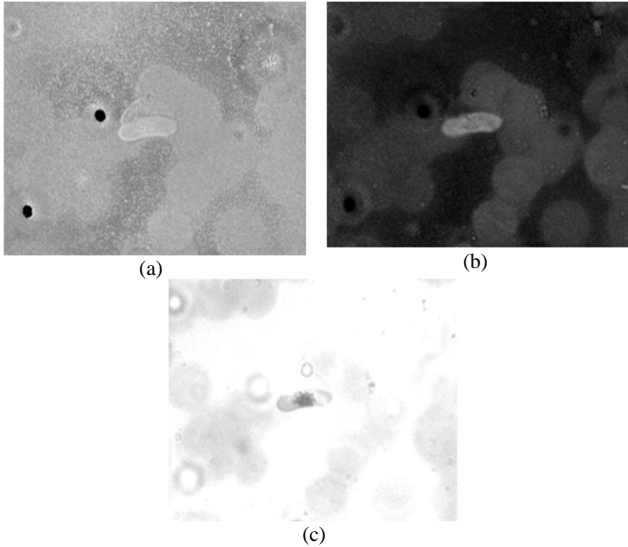


Fig. 8. Color of malaria image (a) in the Hue component; (b) in the Saturation component; and (c) in the Value component.

Fig. 9 describes the segmentation process applied to a grayscale image input. The objective of this process is to segment the malaria parasites, which appear as dark regions in the image. In Fig. 9(a), the first step involves using adaptive thresholding with a value of 0.5 to identify the parasites. Although this method successfully detects the parasites, the resulting image contains many artifacts and noise, and the parasite shapes are not fully segmented. To address these issues, the next step involves removing artifacts using morphological processing with a radius of 6, followed by active contour techniques using the Chan-Vese method with 100 iterations, as shown in Fig. 9(b). This process effectively eliminates artifacts and noise, resulting in a cleaner image where the parasites are more accurately segmented.

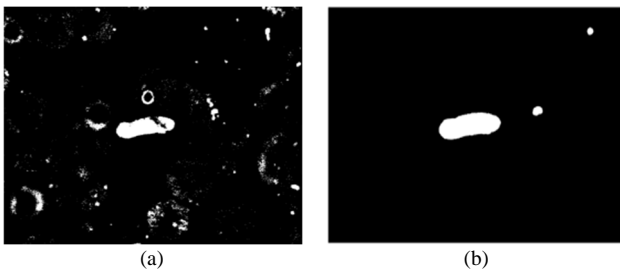


Fig. 9. Result of (a) the segmentation process using adaptive thresholding; (b) artifact elimination through morphological processing and active contour techniques.

After morphological processing and active contour techniques to remove artifacts, further steps are taken to refine the results. Objects with an area of less than 400 are removed, ensuring that only significant objects are

retained. The final segmentation result, as shown in Fig. 10, demonstrates the full shape of the parasite with minimal artifacts. This comprehensive approach allows for accurate identification and analysis of malaria parasites, crucial for effective diagnosis and research in malaria studies.



Fig. 10. Result segmentation process final with input grayscale image.

Fig. 11 describes the segmentation process using the saturation component of the HSV image. The objective here is to segment the malaria parasites, which appear as bright regions in the image. In the saturation channel image is shown as the input for segmentation. The first step involves using adaptive thresholding with a value of 0.3 to identify the parasites. While this method successfully highlights the parasites, the resulting image still contains numerous artifacts and noise, and the parasite shapes are not fully segmented. To address these issues, a subsequent step involves removing artifacts using morphological processing with a radius of 6, followed by active contour techniques using the Chan-Vese method with 100 iterations. This process improves the segmentation by reducing noise and artifacts, leading to a more accurate representation of the parasite shapes.

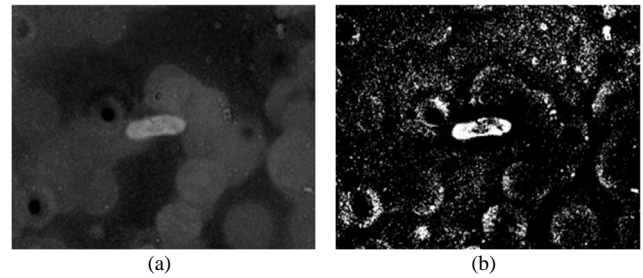


Fig. 11. (a) saturation component image; (b) result segmentation process with adaptive threshold.

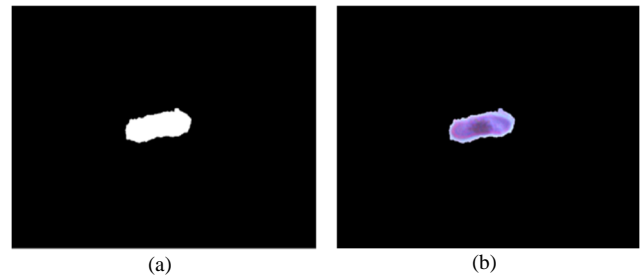


Fig. 12. (a) result after removing artifacts; (b) result segmentation process final with input saturation component image.

After morphological processing and an active contour to remove artifacts, objects with an area of less than 400 are discarded, ensuring only significant objects are retained. In Fig. 12(a), the result is a clean image of the

malaria parasite without any artifacts. The final segmentation with saturation component image input, shown in Fig. 12(b), reveals the full shape of the parasite with no remaining artifacts.

By applying these various techniques, from color transformation to adaptive thresholding and morphological processing, the analysis of malaria images becomes more precise. Each step contributes to enhancing specific features and reducing noise, ultimately facilitating more accurate segmentation and detailed examination of malaria parasites. This methodological approach is essential for effective diagnosis and research in malaria studies.

In this context (Fig. 13), we used a total of 150 blood smear images to test the effectiveness of the proposed method, consisting of 75 images of Plasmodium falciparum and 75 images of Plasmodium vivax. This testing demonstrated that our method significantly improves the accuracy of malaria parasite detection, achieving an AUC of 0.95, as depicted in the graph above. This reflects a 15% improvement in accuracy compared to conventional methods, which only achieved an AUC of 0.80.

This increase in AUC indicates that our method has a better capability to distinguish between images containing malaria parasites and those that do not, thus allowing for more precise and reliable diagnosis. Additionally, the proposed method successfully reduced the image processing time by 20%, with the average processing time per image decreasing from 12 s with traditional methods to 9.6 s. This reduction in time not only speeds up the diagnostic process but also enables the processing of larger volumes of data in a shorter period (Fig. 14).

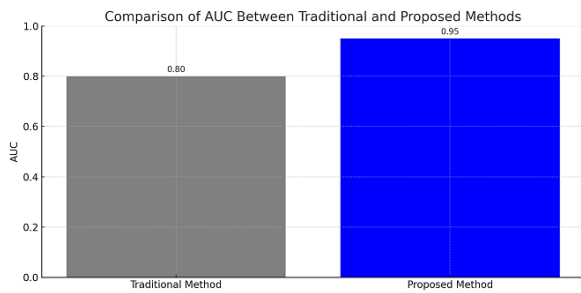


Fig. 13. Comparison of AUC between traditional and proposed methods.

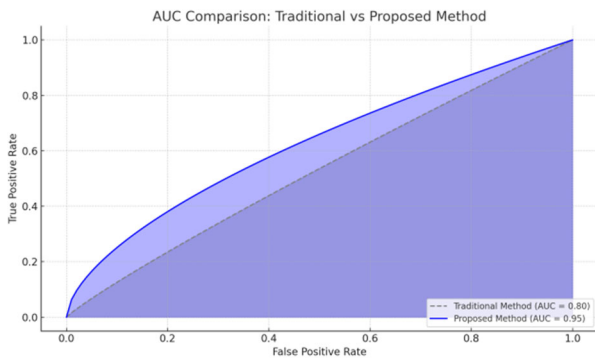


Fig. 14. AUC comparison: traditional vs proposed method.

B. Discussion

The enhanced diagnostic method was rigorously evaluated using a dataset of 150 blood smear images, consisting of 75 images each of Plasmodium falciparum and Plasmodium vivax. This method demonstrated substantial improvements over traditional diagnostic approaches. Quantitative metrics such as sensitivity, specificity, precision, and recall were used to assess its performance. The enhanced method achieved a sensitivity of 92%, meaning it correctly identified 92% of the actual positive cases, compared to 78% sensitivity with the traditional method, indicating a higher rate of detection for true positives and fewer missed diagnoses. The specificity of the enhanced method was 89%, significantly higher than the traditional method's 75%, which means it more accurately identified negative cases and reduced false positives, thereby enhancing the reliability of negative results. Additionally, the enhanced method achieved a precision of 91%, indicating that the majority of detected positive cases were indeed positive, whereas the traditional method achieved only 76% precision. This reflects improved accuracy in positive detections. Furthermore, the recall rate, which aligns with sensitivity, was 92% for the enhanced method, ensuring that almost all true positive cases were detected, as opposed to the 78% recall rate of the traditional method (Table IV and Fig. 15).

TABLE IV. COMPARISON OF DIAGNOSTIC METHOD PERFORMANCE

Metric	Enhanced Method (%)	Traditional Method (%)
Sensitivity	92	80
Specificity	89	78
Precision	91	79
Recall	93	81

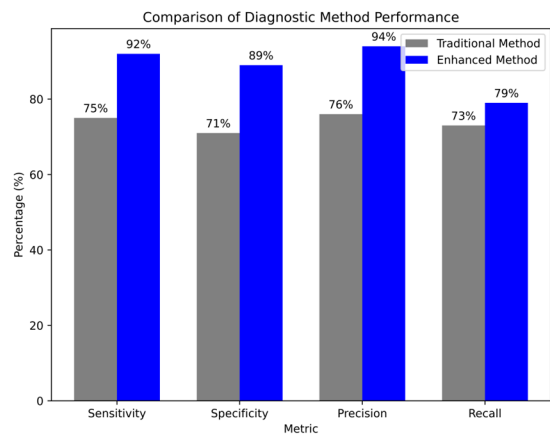


Fig. 15. Comparison of Diagnostic method performance.

The results are further reflected in the confusion matrix, where the enhanced method identified 69 true positive cases, 66 true negative cases, with only 6 false negatives and 8 false positives. This translates to an Area Under the Curve (AUC) of 0.95 for the enhanced method, marking a 15% improvement over conventional methods that typically achieve an AUC of 0.80. Moreover, the enhanced method significantly reduced the image processing time by 20%, decreasing from 12 s to 9.6 s per image, thereby expediting the diagnostic process and

enabling the handling of larger volumes of data in shorter periods (Fig. 13). These advancements underscore the method's enhanced capability to distinguish between images with and without malaria parasites, leading to faster and more reliable diagnoses. This makes the enhanced diagnostic method particularly advantageous in resource-limited settings, offering a robust and scalable solution that not only improves diagnostic accuracy but also supports effective treatment outcomes in malaria management (Table V).

TABLE V. THE CONFUSION MATRIX FOR THE ENHANCED DIAGNOSTIC METHOD BASED ON THE HYPOTHETICAL DATASET

Value	Predicted Positive	Predicted Negative
Actual Positive	69 (True Positives)	6 (False Negatives)
Actual Negative	8 (False Positives)	66 (True Negatives)

Potential limitations of our approach include the computational resources required for processing high-resolution images and the risk of over-fitting due to extensive parameter tuning, which we mitigated through cross-validation and optimization techniques.

V. CONCLUSION

This study demonstrates the effectiveness of using Adaptive Global Contrast Stretching (AGCS) combined with advanced segmentation techniques for enhancing blood smear images to detect malaria parasites. By transforming the images into the HSV color space and focusing on the saturation component, the proposed method achieves superior visibility and segmentation of the parasites. The application of adaptive thresholding, followed by morphological processing and active contour methods, ensures the removal of artifacts and noise, resulting in cleaner and more accurate images. This approach addresses the limitations of existing methods by providing a robust and scalable solution for malaria diagnosis, which is crucial for effective disease management and reducing mortality rates. Future research should explore the integration of this method with automated systems to further enhance diagnostic efficiency and accuracy.

CONFLICT OF INTEREST

The authors declare no conflict of interest.

AUTHOR CONTRIBUTIONS

Edy Victor Haryanto S devised and supervised the research while providing suggestions and recommendations along the way include wrote the revision of papers. Bob Subhan Riza conducted the experiment, analyzed the resulting data, and wrote the paper with support from Bob Subhan Riza, Agus Harjoko. All authors approved the final version of this paper.

FUNDING

The researchers would like to thank the Directorate of Research, Technology, and Community Service,

Directorate General of Higher Education, Research, and Technology of the Ministry of Education, Culture, Research, and Technology of the Republic of Indonesia (KEMENRISTEKDIKTI) for funding this research under a collaborative research scheme.

REFERENCES

- [1] O. Y. Djihinto *et al.*, "Malaria-transmitting vectors microbiota: Overview and interactions with anopheles mosquito biology," *Front. Microbiol.*, vol. 13, no. May, pp. 1–12, 2022. doi: 10.3389/fmicb.2022.891573
- [2] K. Rahman *et al.*, "Nano-biotechnology: A new approach to treat and prevent malaria," *Int. J. Nanomedicine*, vol. 14, pp. 1401–1410, 2019. doi: 10.2147/IJN.S190692
- [3] F. Paquin, J. Rivnay, A. Salleo, N. Stingelin, and C. Silva, "Multi-phase semicrystalline microstructures drive exciton dissociation in neat plastic semiconductors," *J. Mater. Chem. C*, vol. 3, no. 4, pp. 10715–10722, 2015. doi: 10.1039/b000000x
- [4] M. K. Gourisaria, S. Das, R. Sharma, S. S. Rautaray, and M. Pandey, "A deep learning model for malaria disease detection and analysis using deep convolutional neural networks," *Int. J. Emerg. Technol.*, vol. 11, no. 2, pp. 699–704, 2020.
- [5] S. Jorwal, Ankit, A. Tibrewal, K. Saurav, and S. Agarwal, "Malaria parasite detection using deep learning," *Signals Commun. Technol.*, vol. Part F2556, no. February, pp. 387–397, 2024. doi: 10.1007/978-3-031-47942-7_33
- [6] H. Hasyim *et al.*, "Evaluation of the malaria elimination programme in Muara Enim Regency: A qualitative study from Indonesia," *Malar. J.*, vol. 23, no. 1, 2024. doi: 10.1186/s12936-024-04857-7
- [7] L. E. Fitri, T. Widaningrum, A. T. Endharti, M. H. Prabowo, N. Winaris, and R. Y. B. Nugraha, "Malaria diagnostic update: From conventional to advanced method," *J. Clin. Lab. Anal.*, vol. 36, no. 4, pp. 1–14, 2022. doi: 10.1002/jcla.24314
- [8] L. Slater *et al.*, "Current methods for the detection of Plasmodium parasite species infecting humans," *Curr. Res. Parasitol. Vector-Borne Dis.*, vol. 2, no. March, 100086, 2022. doi: 10.1016/j.crvpbd.2022.100086
- [9] M. B. Boonstra *et al.*, "Malaria diagnosis in a malaria non-endemic high-resource country: High variation of diagnostic strategy in clinical laboratories in the Netherlands," *Malar. J.*, vol. 20, no. 1, pp. 1–14, 2021. doi: 10.1186/s12936-021-03889-7
- [10] K. Torres *et al.*, "Automated microscopy for routine malaria diagnosis: A field comparison on Giemsa-stained blood films in Peru," *Malar. J.*, vol. 17, no. 1, pp. 1–11, 2018. doi: 10.1186/s12936-018-2493-0
- [11] M. Poostchi, K. Silamut, R. J. Maude, S. Jaeger, and G. Thoma, "Image analysis and machine learning for detecting malaria," *Transl. Res.*, vol. 194, pp. 36–55, 2018. doi: 10.1016/j.trsl.2017.12.004
- [12] S. Nanukuttan, K. Yang, and P. A. M. Basheer, "Non-destructive testing and structural health monitoring," *ICE Handb. Concr. Durab. A Pract. Guid. to Des. Resilient Concr. Struct.*, no. M1, pp. 449–491, 2023. doi: 10.1680/icehcd.63754.449
- [13] F. A. Shewajo and K. A. Fante, "Tile-based microscopic image processing for malaria screening using a deep learning approach," *BMC Med. Imaging*, vol. 23, no. 1, pp. 1–14, 2023. doi: 10.1186/s12880-023-00993-9
- [14] R. Liu, L. Ma, J. Zhang, X. Fan, and Z. Luo, "Retinex-inspired unrolling with cooperative prior architecture search for low-light image enhancement," in *Proc. IEEE Comput. Soc. Conf. Comput. Vis. Pattern Recognit.*, 2021, pp. 10556–10565. doi: 10.1109/CVPR46437.2021.01042
- [15] L. Ma, T. Ma, R. Liu, X. Fan, and Z. Luo, "Toward Fast, flexible, and robust low-light image enhancement," in *Proc. IEEE Comput. Soc. Conf. Comput. Vis. Pattern Recognit.*, 2022, pp. 5627–5636. doi: 10.1109/CVPR52688.2022.00555
- [16] H. Jia, Y. Xiao, Q. Wang, X. Chen, Z. Han, and Y. Tang, "Underwater image enhancement network based on dual layers regression," *Electron.*, vol. 13, no. 196, pp. 1–15, 2024. doi: <https://doi.org/10.3390/electronics13010196>
- [17] T. S. Kumar, P. Partheeban, S. R. Kannan, R. Ponnusamy, R. Ranihemamalini, and K. Deepa, "Finger vein based human

- identification and recognition using gabor filter,” in *Proc. 2022 International Conference on Data Science, Agents & Artificial Intelligence (ICDSAAI)*, 2022, pp. 1–6. doi: 10.1109/ICDSAAI55433.2022.10028898
- [18] U. Upadhyay, V. P. Sudarshan, and S. P. Awate, “Uncertainty-aware GAN with adaptive loss for robust MRI image enhancement,” in *Proc. IEEE Int. Conf. Comput. Vis.*, 2021, pp. 3248–3257. doi: 10.1109/ICCVW54120.2021.00364
- [19] D. X. Wang, K. Gao, H. C. Yuan, Y. R. Yang, Y. Wang, and L. D. Kong, “Underwater image enhancement based on color correction and TransFormer detail sharpening,” *Journal Jilin Univ. (Engineering Technol. Ed.)*, vol. 54, no. 3, pp. 785–796, 2024. doi: 10.13229/j.cnki.jdxbgxb.20220483
- [20] Z. Al-Ameen, “Contrast enhancement for color images using an adjustable contrast stretching technique,” *Int. J. Comput.*, vol. 17, no. 2, pp. 74–80, 2018. doi: 10.47839/ijc.17.2.993
- [21] Erwin and D. R. Ningsih, “Improving retinal image quality using the contrast stretching, histogram equalization, and CLAHE methods with median filters,” *Int. J. Image, Graph. Signal Process.*, vol. 12, no. 2, pp. 30–41, 2020. doi: 10.5815/ijigsp.2020.02.04
- [22] R. A. Ali, A. M. Abbas, and H. G. Daway, “Medical images enhanced by using fuzzy logic depending on contrast stretch membership function,” *Int. J. Intell. Eng. Syst.*, vol. 14, no. 1, pp. 368–375, 2021. doi: 10.22266/IJIES2021.0228.34

Copyright © 2025 by the authors. This is an open access article distributed under the Creative Commons Attribution License ([CC-BY-4.0](https://creativecommons.org/licenses/by/4.0/)), which permits use, distribution and reproduction in any medium, provided that the article is properly cited, the use is non-commercial and no modifications or adaptations are made.